

## Chemical Control over Immune Recognition: A Class of Antibody-Recruiting Small Molecules That Target Prostate Cancer

Ryan P. Murelli, Andrew X. Zhang, Julien Michel, William L. Jorgensen, and David A. Spiegel\*

Department of Chemistry, Yale University, 225 Prospect Street, P.O. Box 208107, New Haven, Connecticut 06520-8107

Received August 12, 2009; E-mail: david.spiegel@yale.edu

Prostate cancer is the second leading cause of cancer-related death among the American male population, and it has been predicted that one out of every six American men will develop prostate cancer during their lifetime.<sup>1</sup> Available treatment options, including chemical/surgical castration, radiation therapy, and chemotherapy, are often ineffective against advanced disease and are also often associated with severe side effects.<sup>2</sup> Thus, new approaches to treat prostate cancer are highly desirable. To this end, monoclonal antibody therapies have shown promise;<sup>2</sup> however, no such agent has yet successfully obtained FDA approval for the treatment of prostate cancer. Furthermore, antibody drugs are limited by severe side effects, lack of oral bioavailability, and high cost.<sup>3</sup> Here we describe a novel technology for prostate cancer treatment that we believe could address many of the limitations of currently available therapies and that combines advantages of both small-molecule-based and antibody-based strategies.



**Figure 1.** Schematic depiction of the reported approach to prostate cancer targeting. An antibody-recruiting small molecule (ARM) binds the cell-surface prostate cancer marker prostate-specific membrane antigen (PSMA), thus recruiting antibodies to these cells for recognition and targeted killing by the immune system. The bifunctional ARMs are composed of an antibody-binding terminus (ABT), a linker region, and a cell-binding terminus (CBT).

The key component of our approach is what we call antibody-recruiting small molecules targeting prostate cancer (ARM-Ps). These are bifunctional materials capable of redirecting antibodies already present in the human bloodstream to prostate cancer cell surfaces and increasing the destruction of cancer cells by effector cells of the immune system (Figure 1). As shown, ARMs are composed of an antibody-binding terminus (ABT), a cell-binding terminus (CBT), and a linker region. In this manuscript, it is demonstrated that ternary complexes formed between ARM-Ps, human prostate cancer cells (LNCaP cells), and antibodies recognizing the 2,4-dinitrophenyl (DNP) group lead to targeted cell-mediated cytotoxicity of LNCaP cells. The power of this approach derives from the observation that anti-DNP antibodies are already found in the human bloodstream in a high percentage of the human population<sup>4</sup> and are competent to mediate target-cell killing.<sup>5,6</sup> Several approaches that utilize bifunctional materials to recruit antibodies to human pathogens have appeared,<sup>7</sup> but ARM-Ps are the first class of antibody-recruiting small molecules that target prostate cancer. The general strategy reported herein has the potential to initiate novel directions in treating cancer and other diseases.

Our first goal in constructing ARM-Ps was to design an appropriate CBT, and to this end, we chose to target the prostate-

specific membrane antigen (PSMA). PSMA is a cell-surface protein that is highly overexpressed on prostate cancer cells relative to normal cells of the prostate, and its expression increases with clinical stage.<sup>8</sup> This protein has been exploited as a target in both prostate cancer imaging<sup>9</sup> and monoclonal antibody therapy for the disease.<sup>10</sup>

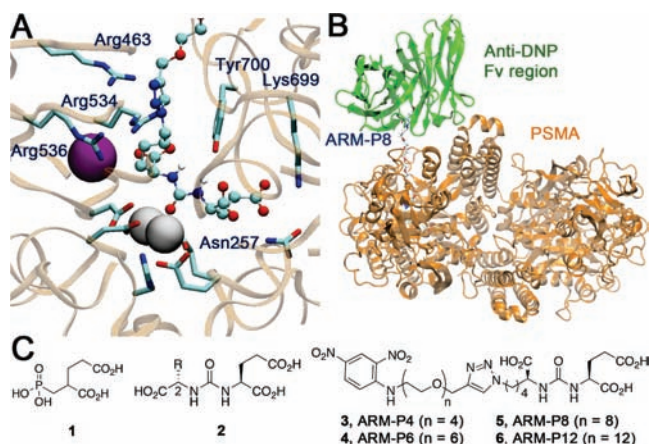


**Figure 2.** Structure-based design studies. (A) Modeled complex illustrating the design of a CBT for use in ARM-Ps. (B) Structural model of the ternary complex between the Fv region of an anti-DNP antibody, ARM-P, and the PSMA dimer. (C) Known PSMA-binding small molecules and structures of ARM-P derivatives utilized in this study. (A) and (B) were created with the program VMD.<sup>11</sup>

Several small-molecule ligands have been developed that bind PSMA selectively and with high affinity, including 2-PMPA (**1**)<sup>12</sup> and the glutamate ureas (**2**) (Figure 2C).<sup>13</sup> These compounds competitively inhibit PSMA's enzymatic activity and have been successfully modified for imaging and targeted drug delivery applications.<sup>14</sup> At the outset of our studies, we were intrigued by observations that **2** could accommodate a wide range of R groups at C2, including various alkyl heterocycle substituents, with minimal loss of inhibitory potency.<sup>13</sup> We therefore reasoned that we might be able to incorporate a linker to join the ABT and CBT at this position.

Thus, starting from a crystal structure for the complex of PSMA with **1**,<sup>15</sup> the corresponding complex with **2** (R = H) was modeled using the program BOMB (biochemical and organic model builder).<sup>16</sup> Stabilizing interactions with active-site zinc ions were indicated, as well as hydrogen bonding and salt-bridge interactions with Tyr700, Lys699, Arg534, Arg536, and Asn257 (Figure 2A). This model was found subsequently to be consistent with the recently published cocrystal structure of PSMA complexed with urea-based ligands.<sup>17</sup> Next, BOMB was used to construct complexes of **2** with alternative DNP linking groups. Among plausible designs, 1-butyl-4-alkyl-1,2,3-triazole analogues (e.g., **3–6**) were judged as promising because of favorable electrostatic interactions with

Arg463,  $\pi$ -stacking interactions with Tyr700, the orientation of the linker toward the solvent, and ease of synthesis.

To estimate viable linker lengths, ternary complexes (involving PSMA, ARM-Ps, the Fv region of an anti-DNP antibody<sup>18</sup>) were constructed using the program FIRST (Figure 2B).<sup>19</sup> Constrained geometric simulations<sup>20</sup> were then performed to assemble the complex with the ABT and CBT binding sites in close proximity. The modeling suggested that at least six oxyethylene units would be necessary to prevent steric clashes between the two proteins and that longer linkers might be preferable to prevent excessive dehydration of the protein–protein interface.

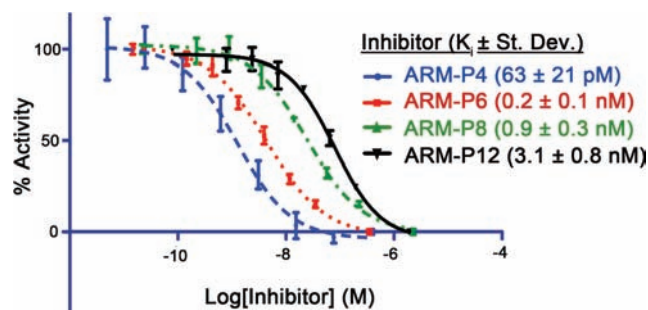


**Figure 3.** Representative PSMA inhibition curves for ARM-Ps.  $K_i$  values were calculated from measured  $IC_{50}$  and  $K_M$  values through the Cheng–Prusoff equation<sup>21</sup> and are reported as the average of three runs  $\pm$  standard deviation.

Thus, ARM-Ps 3–6 were synthesized (Figure 2C; these are called ARM-P4 through ARM-P12 for the number of oxyethylene units in the linker) and tested for binding to PSMA through a standard enzymatic inhibition assay.<sup>22</sup> This assay measures the ability of designed small molecules to inhibit PSMA-catalyzed cleavage of the peptide substrate *N*-acetylasparylglutamate (NAAG). As depicted in Figure 3, compound 3 (ARM-P4) inhibited PSMA with a  $K_i$  of 63 pM, a value similar to that of the most potent PSMA-binding small molecule developed to date.<sup>17</sup> Although we anticipated that the flexible PEG linker in 3 could lead to entropic penalties in binding PSMA, perhaps stabilizing interactions with the triazole, DNP, and/or PEG portions of ARM-P4 compensate. Interestingly, compounds 4–6, which contain 6, 8, and 12 oxyethylene units, exhibited decreased inhibitory potency relative to 3. The origin of the trend is currently under investigation.

To evaluate the capacity of ARM-P derivatives to template ternary complex formation in a cellular environment, we performed live-cell flow cytometry assays with PSMA-expressing LNCaP cells and Alexa Fluor 488-conjugated anti-DNP antibodies. Since the anti-DNP antibody represented the fluorescent component in these studies, rightward shifts of flow cytometry histograms indicate increased levels of ternary complex formation. These experiments revealed an intriguing trend (Figure 4A): although ARM-P4 (3) possessed the highest affinity in PSMA-binding assays, maximal amounts of ternary complex were formed in the presence of ARM-P8 (5). These results are consistent with the predictions of the computational modeling studies (see Figure 2B, above), which suggested that linker lengths  $n = 4$  and 6 could lead to unfavorable steric interactions between the antibody and PSMA. The relative decrease in ternary complex formation for ARM-P12 versus ARM-P8 may simply result from the decreased affinity of ARM-P12 for PSMA, consistent with results in Figure 3.

ARM-P8 was therefore chosen for evaluation in subsequent studies. Flow cytometry experiments performed with an excess of the competing ligand 2-PMPA or bis-DNP lysine (Figure 4B), revealed baseline levels of ternary complex. Furthermore, no ternary

complex formation was observed under these conditions using DU145 prostate cancer cells, which lack PSMA.<sup>23</sup> Together, these data confirm that small-molecule-mediated antibody recruitment is dependent upon binding of ARM-P8 to both PSMA and anti-DNP antibodies. Moreover, competition with 2-PMPA and bis-DNP lysine was found to be concentration-dependent (Figure 4C). The  $K_i$  value determined for 2-PMPA in these studies was found to be 5.0 nM, which is almost identical to that determined in enzymatic assays (2.3 nM).<sup>23</sup> This result implies that ARM-P binding to PSMA does not benefit from increased affinity due to multivalent presentation.<sup>7g,h</sup> Fluorescence microscopy experiments (Figure 4D) further confirmed the flow cytometry data and demonstrated localization of the ternary complex to the cell membrane. No fluorescence was observed in the absence of ARM-P8.<sup>23</sup> Endocytosis of fluorescent features at 37 °C but not 4 °C is consistent with the reported behavior of PSMA.<sup>24</sup>

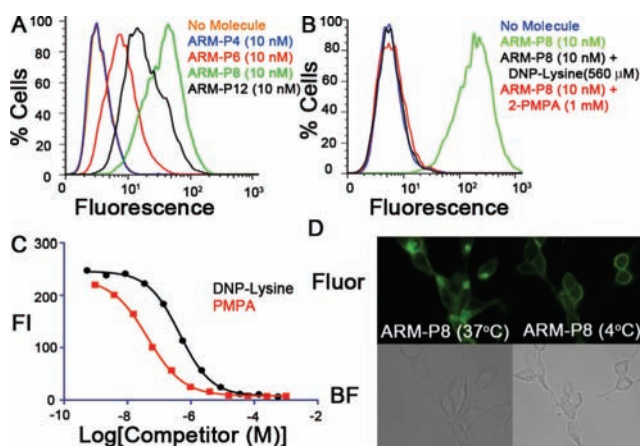


**Figure 4.** Evaluating ternary complex formation. (A, B) Representative traces from flow cytometry experiments. (C) Dose dependence of competitor concentration on ternary complex formation. (D) Epifluorescence (Fluor) and bright-field (BF) microscopy experiments performed in the presence of ARM-P8 at 37 and 4 °C.

Having established that ARM-P8 possessed optimal linker length for forming ternary complexes, we tested its ability to induce cell-mediated cytotoxicity of LNCaP prostate cancer cells. This process is known to take place by way of interactions between Fc receptors on cytotoxic effector cells contained in peripheral blood (such as NK cells, macrophages, and dendritic cells) and the Fc (constant) regions of antibodies.<sup>6</sup> Thus, LNCaP cells were combined with peripheral blood mononuclear cells (PBMCs), anti-DNP antibodies, and ARM-P8, and cell death was measured using a commercially available calcein-release assay (Figure 5).<sup>25</sup> As expected (see below), ARM-P8 at concentrations up to 30 nM led to enhanced cell killing, while treatment with ARM-P4 led to no change in cell viability. The antibody concentration employed in these experiments was slightly below that found in human serum,<sup>4</sup> and lower concentrations were also found to be efficacious (Figure S5 in the Supporting Information). ARM-P8-mediated cell killing was not observed in DU145 cells or in the presence of 2-PMPA, which suggests that the molecular target in these experiments is PSMA (Figure S5). Also, no cytotoxicity was observed in either LNCaP or DU145 cells after treatment with ARM-P8 in the absence of effector PBMCs, indicating that this compound is not itself cytotoxic (Figure S5).

Notably, the intriguing bell-shaped pattern observed in the cell-killing measurements with ARM-P8 has been observed in various situations in which bifunctional ligands template ternary linkages.<sup>26</sup> Such behavior results from the binding dynamics of these systems:

at large total concentrations of the bifunctional small molecule, unbound material competes with the ternary complex, driving the system toward formation of binary complexes. We view this self-antagonistic trend in ARM-P8-mediated cytotoxicity experiments as evidence that cell killing proceeds via reversible formation of a ternary complex. Furthermore, from a clinical standpoint, such a model reveals a unique advantage associated with this novel class of bifunctional therapeutics: they are autoinhibitory and could serve clinically as the antidote for their own overdose.

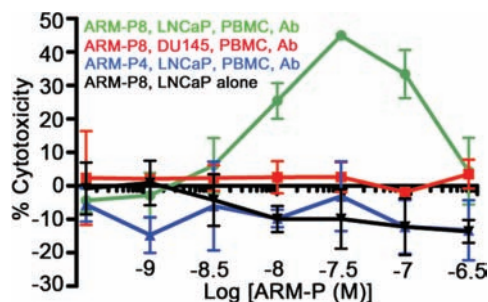


**Figure 5.** Antibody-dependent cellular cytotoxicity assays. LNCaP (PSMA-positive) and DU145 (PSMA-negative) cells were treated with the ARM-P derivatives at the indicated concentrations, and cell death was measured with and without exposure to anti-DNP antibody (Ab, 24  $\mu\text{g}/\text{mL}$ ) and peripheral blood mononuclear cells (PBMC). Points represent the average of four measurements  $\pm$  standard deviation. All depicted trends were observed on at least three separate occasions.

In summary, we have reported the structure-based design of a class of prostate cancer-targeted antibody-recruiting small molecules (ARM-Ps) capable of binding to prostate-specific membrane antigen with high affinity (pM to nM) and recruiting antibodies to PSMA-expressing cells. We have also demonstrated that one member of this class, ARM-P8, is capable of inducing antibody- and PBMC-dependent cytotoxicity at concentrations in the nanomolar range. This ARM-based strategy could have profound advantages in the treatment of human cancers. Its autoinhibitory pharmacology (see Figure 5, above) represents a unique regulatory mechanism worthy of further study. Also, it exploits pre-existing immune mechanisms rather than cytotoxic compounds in cell killing and thus could lead to safer cancer therapies.

**Acknowledgment.** The authors thank John Hines, Thomas Gniadek, and Jacob Appelbaum for helpful suggestions and experimental assistance. This work was funded by the National Institutes of Health through the NIH Director's New Innovator Award Program (DP22OD002913 to D.A.S.) and the National Foundation for Cancer Research (W.L.J.). J.M. acknowledges support from a Marie Curie International Fellowship from the European Commission (FP7-PEOPLE-2008-4-1-IOF, 234796-PPIdesign).

**Supporting Information Available:** Detailed experimental procedures and compound characterization. This material is available free of charge via the Internet at <http://pubs.acs.org>.

## References

- (1) American Cancer Society. Cancer Facts and Figures 2009. [http://www.cancer.org/docroot/STT/content/STT\\_1x\\_Cancer\\_Facts\\_Figures\\_2009.asp](http://www.cancer.org/docroot/STT/content/STT_1x_Cancer_Facts_Figures_2009.asp) (accessed Oct 27, 2009).
- (2) Olson, W. C.; Heston, W. D.; Rajasekaran, A. K. *Rev. Recent Clin. Trials* **2007**, *2*, 182.
- (3) Allen, T. M. *Nat. Rev. Cancer* **2002**, *2*, 750.
- (4) Antibodies recognizing the DNP epitope have been estimated to constitute 1% of circulating IgM ( $\sim 10 \mu\text{g}/\text{mL}$  in human serum) and 0.8% of circulating IgG (40–120  $\mu\text{g}/\text{mL}$  in human serum). See: (a) Karjalainen, K.; Makela, O. *Eur. J. Immunol.* **1976**, *6*, 88. (b) Farah, F. S. *Immunology* **1973**, *25*, 217. (c) Rowe, D. S.; Anderson, S. G.; Skegg, J. In *Immunoglobulins*; Merler, E., Ed.; National Academy of Sciences Press: Washington, DC, 1970; p 361. The prevalence of anti-DNP antibodies has been estimated at 18–90% of humans. See: (d) Ortega, E.; Kostovetzky, M.; Larralde, C. *Mol. Immunol.* **1984**, *21*, 883. (e) Jormalainen, S.; Makela, O. *Eur. J. Immunol.* **1971**, *1*, 471.
- (5) Muller-Eberhard, H. J. *Annu. Rev. Biochem.* **1988**, *57*, 321.
- (6) Hale, G.; Clark, M.; Waldmann, H. J. *Immunol.* **1985**, *134*, 3056.
- (7) For anti-HIV approaches, see: (a) Parker, C. G.; Domaal, R. A.; Anderson, K. S.; Spiegel, D. A. *J. Am. Chem. Soc.* [Online early access]. DOI: 10.1021/ja9057647. Published Online: Oct 19, 2009. (b) Shokat, K. M.; Schultz, P. G. *J. Am. Chem. Soc.* **1991**, *113*, 1861. (c) Naicker, K. P.; Li, H.; Heredia, A.; Song, H.; Wang, L. *Org. Biomol. Chem.* **2004**, *2*, 660. (d) Perdomo, M. F.; Levi, M.; Ilberg, M. S.; Vahlne, A. *Proc. Natl. Acad. Sci. U.S.A.* **2008**, *105*, 12515. For antibacterial approaches, see: (e) Bertozzi, C. R.; Bednarski, M. D. *J. Am. Chem. Soc.* **1992**, *114*, 5543. (f) Bertozzi, C. R.; Bednarski, M. D. *J. Am. Chem. Soc.* **1992**, *114*, 2242. (g) Krishnamurthy, V. M.; Quinton, L. J.; Estroff, L. A.; Metallo, S. J.; Isaacs, J. M.; Mizgerd, J. P.; Whitesides, G. M. *Biomaterials* **2006**, *27*, 3663. For anticancer approaches, see: (h) Carlson, C. B.; Mowery, P.; Owen, O. M.; Dykhuizen, E. C.; Kiessling, L. L. *ACS Chem. Biol.* **2007**, *2*, 119. (i) Popkov, M.; Gonzalez, B.; Sinha, S. C.; Barbas, C. F., III. *Proc. Natl. Acad. Sci. U.S.A.* **2009**, *106*, 4378. (j) Lu, Y.; You, F.; Vlahov, I.; Westrick, E.; Fan, M.; Low, P. S.; Leamon, C. P. *Mol. Pharmaceutics* **2007**, *4*, 695.
- (8) Holmes, E. H.; Greene, T. G.; Tino, W. T.; Boynton, A. L.; Aldape, H. C.; Misrock, S. L.; Murphy, G. P. *Prostate Suppl.* **1996**, *7*, 25.
- (9) Mohammed, A. A.; Shergill, I. S.; Vandal, M. T.; Gujral, S. S. *Expert Rev. Mol. Diagn.* **2007**, *7*, 345.
- (10) Slovins, S. F. *Expert Opin. Ther. Targets* **2005**, *9*, 561.
- (11) Humphrey, W.; Dalke, A.; Schulten, K. *J. Mol. Graph.* **1996**, *14*, 33.
- (12) Slusher, B. S. *Nat. Med.* **1999**, *5*, 1396.
- (13) Kozikowski, A. P.; Zhang, J.; Nan, F.; Petukhov, P. A.; Grajkowska, E.; Wroblewski, J. T.; Yamamoto, T.; Bzdega, T.; Wroblewska, B.; Neale, J. H. *J. Med. Chem.* **2004**, *47*, 1729.
- (14) Humblet, V.; Misra, P.; Bhushan, K. R.; Nasr, K.; Ko, Y.; Tsukamoto, T.; Pannier, N.; Frangioni, J. V.; Maison, W. *J. Med. Chem.* **2009**, *52*, 544.
- (15) Barinka, C.; Rovenska, M.; Mlcochova, P.; Hlouchova, K.; Plechanovova, A.; Majer, P.; Tsukamoto, T.; Slusher, B. S.; Konvalinka, J.; Lubkowsky, J. *J. Med. Chem.* **2007**, *50*, 3267.
- (16) Jorgensen, W. L. *Acc. Chem. Res.* **2009**, *42*, 724.
- (17) Barinka, C.; Byun, Y.; Dusich, C. L.; Banerjee, S. R.; Chen, Y.; Castanares, M.; Kozikowski, A. P.; Mease, R. C.; Pomper, M. G.; Lubkowsky, J. *J. Med. Chem.* **2008**, *51*, 7737.
- (18) James, L. C.; Roversi, P.; Tawfik, D. S. *Science* **2003**, *299*, 1362.
- (19) Jacobs, D. J.; Rader, A. J.; Kuhn, L. A.; Thorpe, M. F. *Proteins* **2001**, *44*, 150.
- (20) Wells, S.; Menor, S.; Hespeneide, B.; Thorpe, M. F. *Phys. Biol.* **2005**, *2*, S127.
- (21) Cheng, Y.; Prusoff, W. H. *Biochem. Pharmacol.* **1973**, *22*, 3099.
- (22) Natarajan, A.; Du, W.; Xiong, C.-Y.; DeNardo, G. L.; DeNardo, S. J.; Gervay-Hague, J. *Chem. Commun.* **2007**, 695.
- (23) Details of these experiments can be found in the Supporting Information.
- (24) Anilkumar, G.; Barwe, S. P.; Christiansen, J. J.; Rajasekaran, S. A.; Kohn, D. B.; Rajasekaran, A. K. *Microwasc. Res.* **2006**, *72*, 54.
- (25) Neri, S.; Mariani, E.; Meneghetti, A.; Cattini, L.; Facchini, A. *Clin. Diagn. Lab. Immunol.* **2001**, *8*, 1131.
- (26) Mack, E. T.; Perez-Castillejos, R.; Suo, Z.; Whitesides, G. M. *Anal. Chem.* **2008**, *80*, 5550, and references therein.

JA906844E